Low-Temperature Fourier Transform Infrared Spectroscopy of Photoactive Yellow Protein†

Yasushi Imamoto,*,‡ Yuji Shirahige,§ Fumio Tokunaga,§ Takamasa Kinoshita,|| Kazuo Yoshihara,⊥ and Mikio Kataoka‡

Graduate School of Materials Science, Nara Institute of Science and Technology, Ikoma, Nara 630-0101, Japan, Department of Earth and Space Science, Graduate School of Science, Osaka University, Toyonaka, Osaka 560-0043, Japan, Department of Chemistry, Faculty of Science, Osaka City University, Sumiyoshi-ku, Osaka 558-8585, Japan, and Suntory Institute for Bioorganic Research, Shimamoto-cho, Osaka 618-8503, Japan

Received January 3, 2001; Revised Manuscript Received June 5, 2001

ABSTRACT: The photocycle intermediates of photoactive yellow protein (PYP) were characterized by low-temperature Fourier transform infrared spectroscopy. The difference FTIR spectra of PYP_B, PYP_H, PYP_L, and PYP_M minus PYP were measured under the irradiation condition determined by UV−visible spectroscopy. Although the chromophore bands of PYP_B were weak, intense sharp bands complementary to the 1163-cm^{-1} band of PYP, which show the chromophore is deprotonated, were observed at 1168−1169 cm^{-1} for PYP_H and PYP_L, indicating that the proton at Glu46 is not transferred before formation of PYP_M. Free *trans-p*-coumaric acid had a 1294-cm^{-1} band, which was shifted to 1288 cm^{-1} in the cis form. All the difference FTIR spectra obtained had the pair of bands corresponding to them, indicating that all the intermediates have the chromophore in the cis configuration. The characteristic vibrational modes at 1020−960 cm^{-1} distinguished the intermediates. Because these modes were shifted by deuterium-labeling at the ethylene bond of the chromophore while labeling at the phenol part had no effect, they were attributed to the ethylene bond region. Hence, structural differences among the intermediates are present in this region. Bands at about 1730 cm^{-1}, which show that Glu46 is protonated, were observed for all intermediates except for PYP_M. Because the frequency of this mode was constant in PYP_B, PYP_H, and PYP_L, the environment of Glu46 is conserved in these intermediates. The photocycle of PYP would therefore proceed by changing the structure of the twisted ethylene bond of the chromophore.

The photoreceptor protein absorbs a photon and then undergoes a protein conformational change. As a result, it acquires a physiologically active conformation. A macromolecule such as protein changes its structure in a stepwise manner, in which distinct elementary reactions are involved. It is therefore important to clarify the structures at each step in order to understand the mechanism for the protein conformational change. The absorbability of visible light to a photoreceptor protein is an advantage for such type of study. Because each state has a distinct chromophore/protein interaction, it is identified as an intermediate on the basis of the absorption spectrum. Thus, the protein conformational change can be detected by following the absorption spectrum of the sample. Among the photoreceptor proteins studied so far, photoactive yellow protein (PYP)[1] (*1*) is one of the most characterized examples.

PYP is a soluble protein that was first discovered in a purple phototrophic bacterium, *Ectothiorhodospira halophila* (*1*). Homologous proteins have since been found in other bacteria (*2*−*6*), and the physiological function is proposed to be a photoreceptor for negative phototaxis against blue light (*7*). PYP of *E. halophila* is composed of 125 amino acids and a *p*-coumaric acid chromophore binding to Cys69 with a thioester bond (*8*−*11*). Accumulated evidence has indicated that the phenolic oxygen of the chromophore in the dark is deprotonated and interacts with Tyr42 and Glu46 by hydrogen bonds. Upon photon absorption, the photocycle is initiated. Our low-temperature spectroscopy has revealed that PYP undergoes a photocycle as follows (*12, 13*):

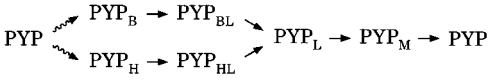

PYP_B and PYP_H are the red-shifted and blue-shifted intermediates, respectively, formed by irradiation at liquid nitrogen temperature. They are thermally converted to PYP_L via PYP_{BL} and PYP_{HL}, respectively. PYP_L is another red-shifted intermediate which is stable at 193 K. PYP_M is a near-UV intermediate trapped at 233 K in PYP dry film.

At room temperature, the intermediates called I0, I0‡, I1 (or pR), and I2 (or pB) were identified (*14*−*17*). The

† This work was supported in part by a Grant-in-Aid for Scientific Research from the Ministry of Education, Culture, Sports, Science, and Technology of Japan, by Kansai Research Foundation for Technology Promotion, and by a SUNBOR grant.

* Correspondence should be addressed to this author. Phone: 81 743 72 6101. Fax: 81 743 72 6109. E-mail: imamoto@ms.aist-nara.ac.jp.

‡ Nara Institute of Science and Technology.

§ Osaka University.

|| Osaka City University.

⊥ Suntory Institute for Bioorganic Research.

[1] Abbreviations: PYP, photoactive yellow protein from *Ectothiorhodospira halophila*; Tris, tris(hydroxymethyl)aminomethane; UV, ultraviolet; FTIR, Fourier transform infrared.

10.1021/bi010021l CCC: $20.00
Published on Web 07/06/2001

spectroscopic properties of I0 and I0‡ suggest that they correspond to PYP_B formed at liquid nitrogen temperature (*18*). On the other hand, I1 and I2 correspond to PYP_L and PYP_M, respectively. Recently we have clarified that the pathway in the early stage at room temperature is also branched (*18*), and the photocycle at room temperature is thought to be essentially similar to that at low temperature. Because PYP is a water-soluble small protein, it is a good target for structural characterization using X-ray crystallography and NMR: the structure of not only PYP in the dark (*19, 20*) but also its intermediates (*21*−*24*) has been studied.

It is widely accepted that the photochemical event in PYP is the isomerization of the chromophore. It was first demonstrated that *p*-coumaric acid released from an intermediate by hydrolysis of the thioester bond had a cis configuration (*25*). Then the chromophore configuration of the intermediates was directly shown by crystallography (*21*−*23*). Although the crystallography is informative, the reaction in the crystal is not necessarily the same as that in the solution. In fact, recent time-resolved FTIR experiments for I1 (PYP_L) suggest that the movement of PYP chromophore on photon absorption in the solution is strikingly different from that in the crystal (*26, 27*). Therefore, the reaction model of PYP proposed on the basis of the crystallography is not definitive, and conventional spectroscopic study using the sample in mild conditions such as in solution and hydrated film is also important.

FTIR spectroscopy is a powerful tool for analysis of the local change of the protein which induces the global conformational change (*28, 29*). It has been demonstrated that Glu46 is protonated in PYP_L (*26, 27*) but the proton at Glu46 is transferred to the chromophore in PYP_M (*13*). Other applications for the glutamic acid, protein backbone, and the water inside the PYP molecule have been reported (*30*−*32*), and numerous data have been accumulated. However, only a few results on FTIR spectroscopy focusing on the early intermediates such as PYP_B and PYP_H have been reported.

To date, both time-resolved and low-temperature FTIR spectroscopy experiments have been performed. In the latter, a PYP sample was cooled and irradiated to trap the intermediate(s). As such, the irradiation temperature and wavelength are crucial to trap the specific intermediate. Our previous low-temperature visible spectroscopy experiments showed that a red-shifted photoproduct is formed at liquid nitrogen temperature (PYP_B), which was distinct from that formed at −80 °C (PYP_L) (*12*). In addition, at liquid nitrogen temperature, a photo-steady-state mixture composed of PYP, PYP_B, and PYP_H is formed. Former application of low-temperature FTIR spectroscopy to PYP lacked consideration about the complicated photoreaction. An FTIR spectrum recorded at 77 K was assigned to PYP_L (pR) (*31, 32*), but it would be the mixture of PYP_B and PYP_H. Therefore, the FTIR spectrum at 77 K should be separated into those of PYP_H and PYP_B to examine their structures.

In the present study, we determined the irradiation condition in the hydrated PYP film to trap each intermediate separately by UV−visible spectroscopy. Under this condition, pure difference FTIR spectra of PYP_B, PYP_H, PYP_L, and PYP_M were obtained. The C═O stretching mode and some of the chromophore bands were assigned using E46Q mutant and deuterium-labeled PYP. In addition, the band specific for *cis*-*p*-coumaric acid was identified. On the basis of these results, the chromophore structures of the intermediates were discussed.

Scheme 1. Synthesis of *p*-Coumaric-2,6-$^2H_2$ Acid (**7**)[a]

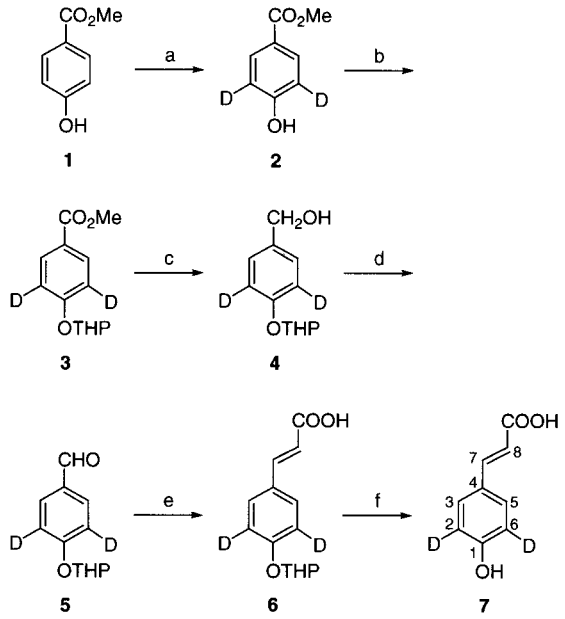

[a] Reagents and conditions: (a) D_2SO_4 in D_2O, room temperature, 5 h; (b) 3,4-dihydropyran, camphorsulfonic acid, CH_2Cl_2, room temperature, 3 h; (c) $LiAlH_4$, ether, boil, 2 h; (d) $(COCl)_2$, dimethyl sulfoxide, trimethylamine, CH_2Cl_2, −78 °C, 30 min; (e) $CH_2(COOH)_2$, pyridine, reflux, 2 h; (f) 5% D_2SO_4 in D_2O, 0 °C, 30 min.

Scheme 2. Synthesis of *p*-Coumaric-8-^2H Acid (**10**)[a]

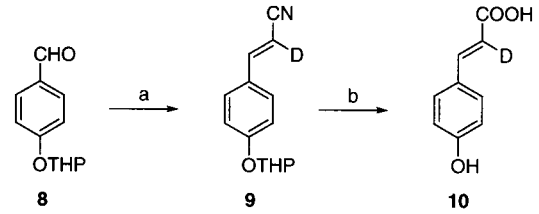

[a] Reagents and conditions: (a) CD_3CN−KOH, reflux, 10 min; (b) dilute H_2SO_4, boil, 2 h.

MATERIALS AND METHODS

Sample Preparation. Wild-type PYP of *Ectothiorhodospira halophila* and its mutant, E46Q, were prepared using a heterologous overexpression system by *Escherichia coli* as reported previously (*33*). They were reconstituted with *p*-coumaric anhydride (*11*) and purified by ammonium sulfate precipitation and DEAE-Sepharose column chromatography (Amersham Pharmacia Biotech).

Deuterium-labeled PYP was reconstituted from apoPYP and deuterium-labeled *p*-coumaric anhydride. ApoPYP was prepared by incubation of purified PYP at 20 °C in the presence of 1 M hydroxylamine and 1 mM dithiothreitol to cleave the thioester bond of the chromophore (*11*). *p*-Coumaric-2,6-$^2H_2$ acid (**7**) and *p*-coumaric-8-^2H acid (**10**) were prepared as shown in Schemes 1 and 2, respectively. 2,6-$^2H_2$-PYP and 8-^2H-PYP were reconstituted and purified by DEAE-Sepharose column chromatography.

For preparation of *cis*-*p*-coumaric acid, 10 mM *trans*-*p*-coumaric acid in aqueous solution at pH 12.0 was irradiated

by 350-nm light obtained by a 1-kW slide projector (HILUX-H_R, Rikagaku Seiki) and a glass band-pass filter (UVD-35, Toshiba) for 16 min. It was lyophilized and dissolved in D_2O, followed by NMR analysis to determine the configuration of ethylene bond.

Spectroscopy. PYP and E46Q were concentrated to 3−4 mg/mL in 10 mM KH_2PO_4-K_2HPO_4 buffer at pH 7.0. A 20 μL aliquot of sample was placed on a BaF_2 window (diameter, 10 mm) and dried under a gentle stream of N_2 gas. To trap PYP_L or $E46Q_L$ at 193 K, 1% glycerol was added to the sample prior to the evaporation to avoid contamination of M intermediate. The sample was hydrated by putting a 0.1 μL drop of H_2O in the sample cell sealed by silicon rubber.

For low-temperature measurements, an Oxford DN1704 optical cryostat connected to ITC502 temperature controller was used. UV−visible spectroscopy and FTIR spectroscopy were carried out using a Hitachi U-3210 recording spectrophotometer and Horiba FT-210 Fourier transform infrared spectrophotometer, respectively. The experimental setup was the same as that reported previously (*13*).

RESULTS

Low-Temperature UV−Visible Spectroscopy of PYP Film. Prior to the FTIR measurements, it is necessary to confirm which irradiation condition yields the aimed at intermediate. Previous low-temperature spectroscopy experiments using PYP in 66% glycerol buffer have shown that PYP_B and PYP_H are formed at −190 °C and PYP_L at −80 °C (*12*). While PYP_M was not trapped at low temperature in a 66% glycerol sample, it was trapped at −40 °C in hydrated film (*13*). PYP_{BL} and PYP_{HL} were thermally formed from PYP_B and PYP_H, respectively, but their isolation was difficult. In the present experiments, the accumulation conditions for PYP_B, PYP_H, PYP_L, and PYP_M in the hydrated film were therefore determined.

At 77 K, the spectral change upon irradiation depended on the irradiation wavelength (Figure 1a,b). Irradiation with 430-nm light caused an absorbance increase at 470−550 nm and a decrease at 350−470 nm. The former was due to the formation of PYP_B, and the latter, to the formation of PYP_H as well as conversion of PYP. The difference spectrum (Figure 1a, inset) was similar to that obtained with the 66% glycerol sample (*12*). Therefore, PYP_B and PYP_H were concluded to have been produced in this irradiation condition. Because PYP, PYP_B, and PYP_H are photoconvertible at 77 K, PYP_B can be converted to PYP and PYP_H. Hydrated PYP film which had been irradiated with 430-nm light (Figure 1b, curve 2) was irradiated with >450-nm light (curves 3−7). By the latter irradiation, absorbance at 470−550 nm decreased and that at 350−460 nm recovered, but the absorption maximum was slightly blue-shifted, indicating the formation of PYP_H. Finally, in the difference absorption spectrum before and after irradiation, the absorbance increase at 480 nm was negligible (Figure 1b, inset). Under this irradiation condition, PYP_H was enriched.

Next, the irradiation condition to trap PYP_L was examined. Because PYP_L is trapped at 193 K in 66% glycerol sample (*12*), we first irradiated a hydrated PYP film with 430-nm light at 193 K. However, this irradiation procedure induced comparable absorbance increases at 470 and 350 nm,

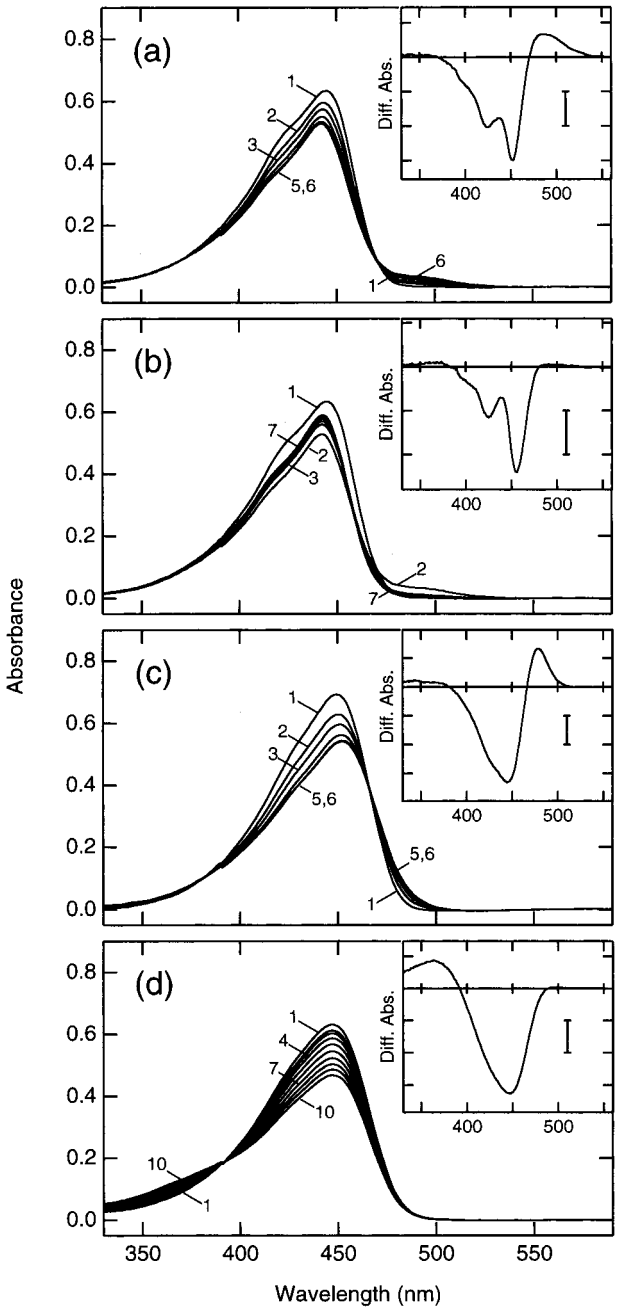

FIGURE 1: Low-temperature spectroscopy of PYP film: (a) PYP film cooled to 77 K (curve 1) and irradiated with 430-nm light for 5, 10, 20, 40, and 80 s (curves 2−6); (b) PYP film cooled to 77 K (curve 1) and irradiated with 430-nm light for 2 min (curve 2), followed by irradiation with >450-nm light for 5, 10, 20, 40, and 80 s (curves 3−7); (c) PYP film containing 1% glycerol cooled to 193 K (curve 1) and irradiated with 430-nm light for 5, 10, 20, 40, and 80 s (curves 2−6); (d) PYP film cooled to 233 K (curve 1) and irradiated with >450-nm light for 5, 10, 20, 40, 80, 160, 320, 640, and 1280 s (curves 2−10). Insets: Difference spectra between the first curves and the last curves. Scale bars represent 0.05 absorbance.

indicating the formation of PYP_M as well as PYP_L (data not shown). PYP_{BL} was stable at the temperature lower than 193 K. Glycerol was then added to the sample to 1% before evaporation, because glycerol inhibits the formation of PYP_M at low temperature (*34*). This sample was dried and hydrated similarly. Irradiation with 430-nm light at 193 K induced a red-shift of the absorption spectra (Figure 1c). The absorbance increase at 475 nm upon irradiation was observed,

but that at 350 nm was very small (Figure 1c, inset), indicating that PYP_L accumulated in this condition. In fact, a clear isosbestic point was observed at 466 nm. PYP_M was trapped by irradiation with >450-nm light at 233 K as shown by the absorbance increase at 360 nm (Figure 1d) (*13*).

FTIR Spectroscopy. Hydrated PYP film was irradiated in the conditions determined by the UV−visible spectroscopy, and the difference FTIR spectra before and after the irradiation were recorded. The sample was irradiated with 430-nm light at 77 K for PYP_H + PYP_B/PYP (Figure 2a) and 430-nm light followed by >450-nm light at 77 K for PYP_H/PYP (Figure 2b). PYP_B/PYP (Figure 2c) was calculated using PYP_H + PYP_B/PYP and PYP_H/PYP on the basis of the subtraction criteria obtained by UV−visible spectroscopy as follows.

The difference UV−visible spectrum in the inset of Figure 1a is the PYP_B plus PYP_H minus PYP spectrum. If the absorption spectra of PYP_B and PYP_H are well-separated from that of PYP, the shape of the negative band would be similar to PYP spectrum. However, the negative band of this spectrum disagrees with the PYP spectrum. The PYP_H spectrum is overlapping on PYP spectrum, while the PYP_B spectrum is 40-nm red-shifted from the PYP spectrum (*12*). Therefore, if the contribution of PYP_H is subtracted from PYP_B + PYP_H/PYP (UV-visible), the shape of the negative band would be similar to PYP spectrum. Various amplitudes of PYP_H/PYP (Figure 1b, inset) were subtracted from PYP_B + PYP_H/PYP (Figure 1a, inset), and the shape of the negative band was compared with the PYP spectrum. The best factor for this criterion was 1.0 (data not shown). PYP_B/PYP (Figure 2c) was thus calculated by subtracting trace b (before normalization) from trace a (before normalization) in Figure 2.

PYP solution containing 1% glycerol was dried, hydrated, and irradiated with 430-nm light at 193 K for PYP_L/PYP (Figure 2d). PYP_M/PYP was obtained by irradiation of the sample without glycerol with >450-nm light at 233 K (Figure 2e).

The C=O stretching modes of glutamic acid or aspartic acid were observed at ~1740 cm^{-1} for PYP and ~1732 cm^{-1} for PYP_H, PYP_B, and PYP_L. We have previously assigned the 1737-cm^{-1} band of PYP in PYP_M/PYP to the C=O stretching mode of protonated Glu46 (*13*). For assignments of complementary positive bands at ~1732 cm^{-1}, FTIR spectra of the E46Q mutant were recorded. Because the lifetimes of the intermediates of E46Q are different from those of wild type (*35*, *36*), formations of the same intermediates as those of wild type were also confirmed by UV−visible spectroscopy using the dry film of E46Q. It was irradiated with 430-nm light at 77 K for formation of the mixture of $E46Q_B$ and $E46Q_H$ (Figure 3a), with 430-nm light followed by >500-nm light at 77 K for formation of $E46Q_H$ (Figure 3b), with 430-nm light at 193 K for formation of $E46Q_L$ (Figure 3c), and with >450-nm light at 233 K for formation of $E46Q_M$ (Figure 3d). The difference UV−visible absorption spectra before and after the irradiation were compared with those of wild type (Figure 3, left panel). The absorption spectra of E46Q intermediates were similar in shape to those of wild type, while they were 10−15 nm red-shifted as in the dark state, indicating that the same intermediates are formed at the same irradiation temperature as that for wild type. The difference FTIR spectra were then recorded similarly (Figure 3a′−3d′). Because the ~1732-cm^{-1} bands for PYP_B plus PYP_H, PYP_H, and PYP_L disappeared in E46Q, they were attributed to Glu46.

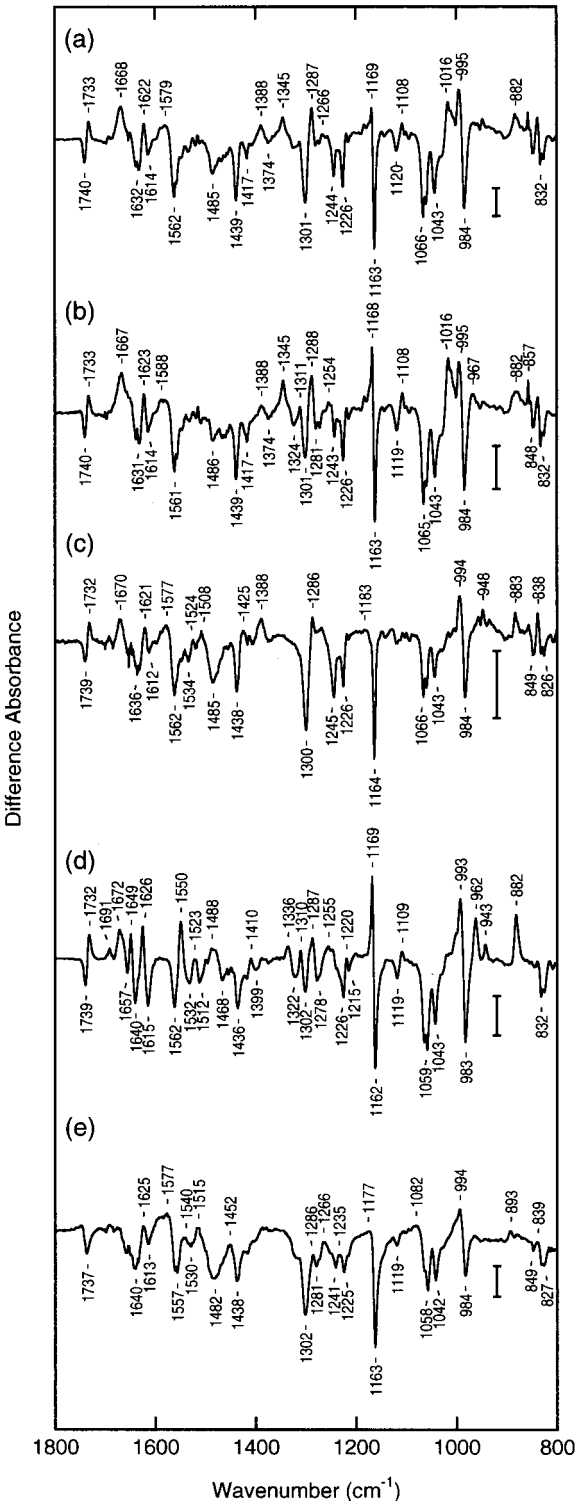

FIGURE 2: Difference FTIR spectra before (negative) and after (positive) the irradiation of PYP. Scale bars represent 0.003 absorbance. The irradiation conditions or calculation were as follows. (a) 430 nm for 2 min at 77 K (PYP_B + PYP_H/PYP); (b) 430 nm for 2 min followed by >450 nm for 2 min at 77 K (PYP_H/PYP); (c) trace a (before normalization) minus trace b (before normalization) (PYP_B/PYP); (d) 430 nm for 3 min at 193 K (PYP_L/PYP); (e) >450 nm for 5 min at 233 K (PYP_M/PYP).

The vibrational modes of the deprotonated chromophore (*37*) were observed at 1482, 1438, and 1163 cm^{-1} for PYP

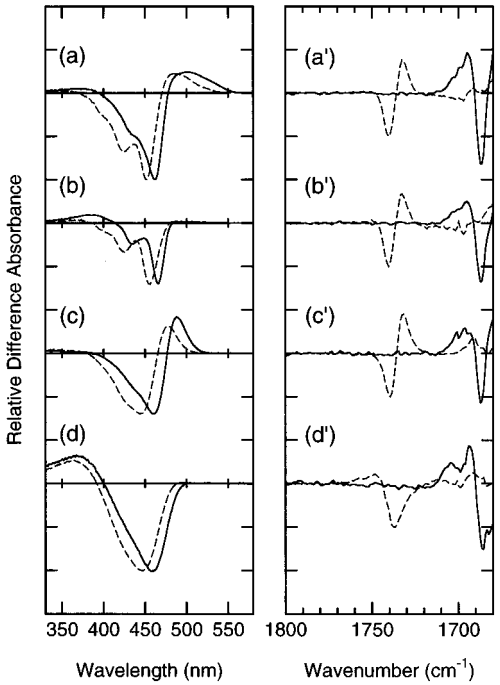

FIGURE 3: Difference UV−visible (a−d) and FTIR spectra (a′−d′) before (negative) and after (positive) the irradiation of E46Q. The irradiation conditions were as follows: (a, a′) 430 nm for 2 min at 77 K ($E46Q_B$ + $E46Q_H$/E46Q); (b, b′) 430 nm for 2 min followed by >500 nm for 2 min at 77 K ($E46Q_H$/E46Q); (c, c′) 430 nm for 3 min at 193 K ($E46Q_L$/E46Q); (d, d′) >450 nm for 5 min at 233 K ($E46Q_M$/E46Q). For comparison, the corresponding spectra of the wild type (broken lines) are superimposed (reproduced from Figures 1 and 2).

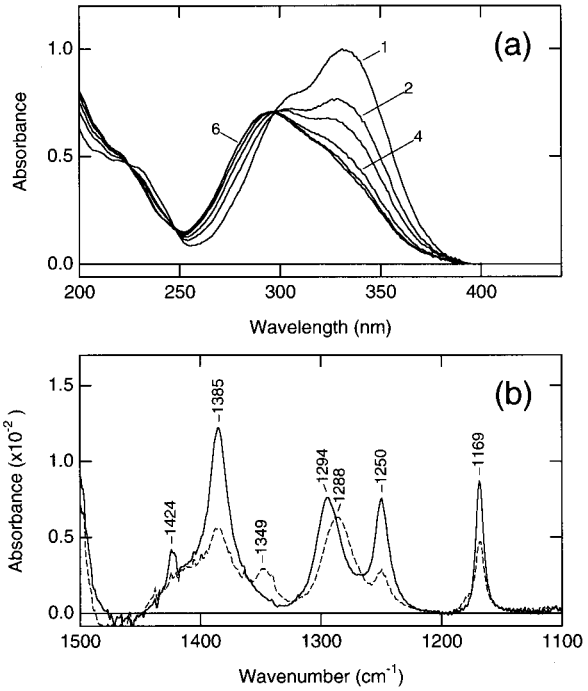

FIGURE 4: UV−visible and infrared absorption spectra of *trans-p*-coumaric acid and its photoproduct: (a) 10 mM *trans-p*-coumaric acid was dissolved in water at pH 12.0 and the UV−visible absorption spectrum was recorded in a 10-μm light path length (curve 1). It was then irradiated with 350-nm light for 1, 2, 4, 8, and 16 min, and the absorption spectra were recorded (curves 2−6, respectively). (b) The infrared absorption spectra of the same sample were recorded before (solid line) and after 350-nm irradiation for 16 min (broken line).

in PYP_M/PYP. Some corresponding bands were observed for the other intermediates. The characteristic bands at 1020−960 cm^{-1} distinguished the intermediates; namely, PYP_H had 1016-, 995-, and 967-cm^{-1} bands, PYP_L had 993- and 962-cm^{-1} bands, and PYP_B and PYP_M had 994-cm^{-1} bands. In PYP_H/PYP, the band at 1016 cm^{-1} is higher than that at 995 cm^{-1}, whereas the latter is higher in PYP_B + PYP_H/PYP. Therefore, the ratio of PYP_H and PYP_B can be estimated from these dual bands. These characteristic bands will be examined in detail in the Discussion.

Spectroscopic Properties of cis-p-Coumaric Acid. To assign the vibrational modes of *p*-coumaric acid specific for the cis form, the spectroscopic properties of free *cis-p*-coumaric acid were studied. *p*-Coumaric acid was dissolved in H_2O, and the pH was adjusted to 12.0. The UV−visible absorption spectra were then recorded (Figure 4a). The phenolic oxygen of the *p*-coumaric acid was deprotonated at pH 12.0 (pK_a = 9.0), and the absorption maximum was located at 332 nm. By irradiation with 350-nm light, the spectrum was blue-shifted with decrease of the extinction coefficient. Finally, absorption maximum shifted to 295 nm.

To confirm the configuration of *p*-coumaric acid, *p*-coumaric acid solutions before and after the irradiation were lyophilized and dissolved in D_2O, followed by NMR analysis. J_{a-b} was 15.62 Hz before irradiation, whereas $J_{a'-b'}$ was 12.69 Hz for the photoproduct (data not shown). These values are in good agreement with those reported previously (*25*), indicating that the photoproduct was in the cis form. The amount of *cis-p*-coumaric acid in this irradiation condition was estimated to be 81% from the band area of NMR signal.

The spectral blue-shift possibly takes place by the protonation of phenolic oxygen. However, the pH titration experiment for *cis-p*-coumaric acid demonstrated that the pK_a of its phenolic oxygen was 10.0 (data not shown), and the population of deprotonated form at pH 12.0 is calculated to be >98%. In addition, the UV−visible spectral change shown in Figure 4a was identical with that observed upon the irradiation of the dilute *p*-coumaric acid solution (~40 μM) buffered by 50 mM Na_2HPO_4 at pH 12.0 (data not shown). Therefore, no protonation of *cis-p*-coumaric acid took place upon our experiment and the difference in FTIR spectra as well as in UV−visible spectra can be attributed to the difference in configuration of the ethylene bond.

The infrared absorption spectra of *trans-* and *cis-p*-coumaric acid were measured by FTIR (Figure 4b). The solution of *trans-p*-coumaric acid was set in the FTIR spectrometer, and the spectrum was measured. It was then irradiated with 350-nm light, and the spectrum measured again. Because the sample was not changed for each measurement, the amplitudes of these two spectra can be compared directly. The trans form had prominent bands at 1424, 1385, 1294, 1250, and 1169 cm^{-1}. Among them, the vibrations corresponding to the 1385- and 1250-cm^{-1} modes have not been observed by the resonance Raman experiment of PYP (*37*). These modes of PYP chromophore would be largely shifted or lost because of the interaction with nearby amino acid residues and/or the formation of the thioester bond. On the other hand, the 1294- and 1169-cm^{-1} modes were detected at 1288 and 1165 cm^{-1}, respectively, by resonance Raman experiment (*37*). The intensity of the 1169-cm^{-1} band was reduced on isomerization, whereas the band

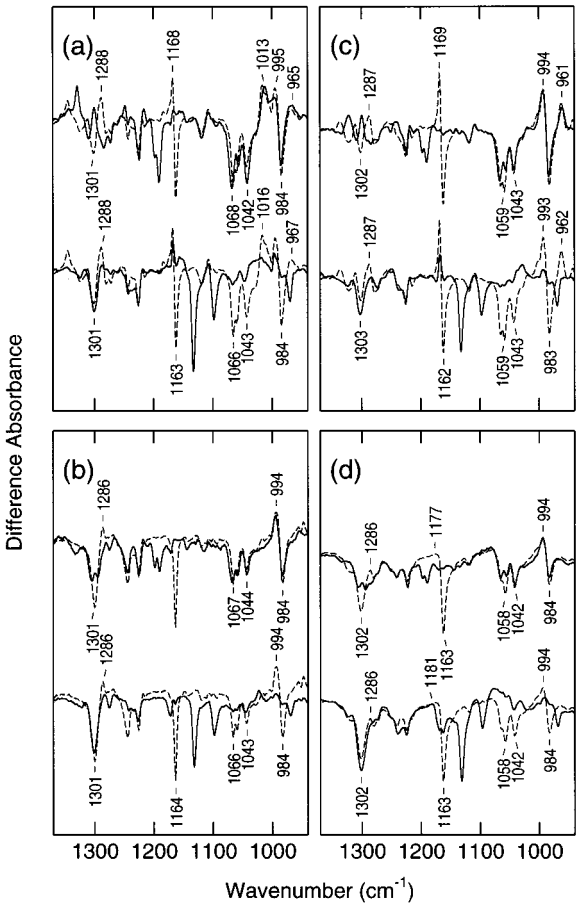

FIGURE 5: FTIR spectroscopy of deuterium-labeled PYP. PYP_H/PYP (a), PYP_B/PYP (b), PYP_L/PYP (c), and PYP_M/PYP (d) in 2,6-$^2H_2$-PYP (top traces) and 8-^{2}H-PYP (bottom traces) are shown. For comparison, those in native PYP are overlapped (dashed line). The experimental conditions were the same as those in Figure 2.

at 1294 cm^{-1} shifted to 1288 cm^{-1}. Therefore, the changes in the vibrational modes of the chromophore on isomerization were considered to be the downshift of the 1294-cm^{-1} band and the intensity decrease of the 1169-cm^{-1} band. The sets of bands at 1288/1301 cm^{-1} for PYP_H/PYP, 1286/1300 cm^{-1} for PYP_B/PYP, 1287/1302 cm^{-1} for PYP_L/PYP, and 1286/1302 cm^{-1} for PYP_M/PYP were observed. They would correspond to the 1288/1294 cm^{-1} band of free *p*-coumaric acid. In addition, the intensities of the 1168- and 1169-cm^{-1} bands of PYP_H and PYP_L were lower than the corresponding band of PYP at 1163 cm^{-1}. This mode was not observed for PYP_B probably because its intensity was very low. The intensity of this mode of PYP_M was also very low although it shifted to 1177 cm^{-1} due to the protonation of the chromophore (*13*, *37*). To confirm that these bands were attributable to the chromophore, the PYP analogues with deuterium-labeled chromophores were prepared and similar measurements were performed (Figure 5).

2,6-$^2H_2$-PYP (upper traces) and 8-^{2}H-PYP (lower traces) were prepared and PYP_H/PYP (panel a), PYP_B/PYP (panel b), PYP_L/PYP (panel c), and PYP_M/PYP (panel d) were recorded similarly. The bands at 1288 and 1168 cm^{-1} of PYP_H, that at 1286 cm^{-1} of PYP_B, those at 1287 and 1169 cm^{-1} of PYP_L, those at 1286 and 1177 cm^{-1} of PYP_M, and those at 1301 and 1163 cm^{-1} of PYP were shifted in 2,6-$^2H_2$-PYP, indicating that these bands were attributable to the chromophore. Therefore, the configuration of the chromophore of PYP is the trans form, whereas those of all intermediates are in the cis forms.

As mentioned above, the characteristic bands at 1020−960 cm^{-1} distinguished the intermediates. These bands were not shifted in 2,6-$^2H_2$-PYP but remarkably shifted in 8-^{2}H-PYP. Therefore, these bands were considered attributable to the ethylene part of the chromophore.

DISCUSSION

In the previous low-temperature FTIR studies which focused on the early stages of the photocycle of PYP, the discrimination of PYP_B and PYP_L and the presence of PYP_H were not considered (*31*, *32*). We therefore studied the irradiation condition at low temperature for formation of the specific intermediate(s) using hydrated PYP film. As a result, the difference FTIR spectra between PYP and its typical intermediates, PYP_H, PYP_B, PYP_L, and PYP_M, were obtained.

UV−visible spectroscopy for PYP_H and PYP_M (Figure 1b,d) clearly demonstrated that neither PYP_B nor PYP_L was formed in these irradiation conditions because no red-shifted intermediate was formed. It is thus reasonable to consider that PYP_H/PYP (Figure 2b) and PYP_M/PYP (Figure 2e) are pure spectra. On the other hand, traces c and d may possibly be mixtures of PYP_B and PYP_H and the mixture of PYP_L and PYP_M, respectively.

PYP_L/PYP was measured at 193 K using the sample supplemented with a small amount of glycerol to inhibit the formation of PYP_M. As a result, the absorbance increase at 350 nm, which demonstrates the formation of PYP_M, was negligible and a clear isosbestic point was observed at 466 nm upon formation of PYP_L. The calculation criteria for PYP_B/PYP were also based on the UV−visible spectra (see Results). Although these irradiation conditions and calculation criteria were obtained independently of FTIR data, one can find the FTIR bands which are characteristic for PYP_H or PYP_M but completely disappear in trace c or d. For example, 1016- and 1345-cm^{-1} bands for PYP_H (trace b) are not found for PYP_B in trace c. Similarly, 1082- and 893-cm^{-1} bands for PYP_M (trace e) are not found for PYP_L in trace d.

In all the difference FTIR spectra except for PYP_M/PYP, clear pairs of bands at ∼1732/1740 cm^{-1} were observed. The 1737-cm^{-1} band of PYP in PYP_M/PYP was assigned to the C═O stretching mode of protonated Glu46 (*13*). The complementary positive bands at ∼1732 cm^{-1} were also attributed to Glu46, because they were not observed when the same experiments were carried out using E46Q mutant (Figure 3). The presence of this mode in PYP_H, PYP_B, and PYP_L indicates that Glu46 is protonated before the formation of PYP_M. It should be noted that this mode of PYP was downshifted on formation of PYP_B and PYP_H but that these were not altered on their conversion to PYP_L. Therefore, the environment of the hydrogen bond of Glu46 is not altered among these intermediates, and Glu46 would not be involved in the structural change on formation of PYP_L. In addition, the UV−visible difference absorption spectra of the E46Q system were 10−15-nm red-shifted from those of wild type while their spectral shapes were similar (Figure 3, left panel). It indicates that like dark-state E46Q, the absorption spectra of E46Q intermediates are also 10−15-nm red-shifted from those of the corresponding intermediates of wild type. The

red-shift of absorption maximum of E46Q relative to wild type is due to the change in the hydrogen bond between the chromophore and Glu46. Therefore, it is reasonable to speculate that Glu46 interacts with the chromophore in the intermediates as well. These findings disagree with the model derived from previous crystallography. Glu46 of PYP_{BL} interacts with the chromophore by a hydrogen bond (*23*), but it does not in PYP_L (*22*). If the partner of the hydrogen bond of Glu46 is changed, the frequency of the C═O stretching mode of Glu46 should be altered. This inconsistency suggests a difference in the reaction mechanism between the crystal and dry film.

Resonance Raman spectroscopy has previously shown that the deprotonated chromophore of PYP has prominent vibrational modes at 1500, 1434, and 1166 cm^{-1}, while the protonated one has instead a vibrational mode at 1176 cm^{-1} (*37*). In PYP_M/PYP, the bands characteristic for the deprotonated chromophore are clearly observed at 1482, 1438, and 1163 cm^{-1} for PYP. Although the 1177-cm^{-1} band for PYP_M was small, the existence of this band is confirmed by the fact that it shifts when PYP having a ^{13}C-labeled chromophore (*13*) or ^{2}H-labeled chromophore is used (Figure 5d). In the present data, pairs of bands were observed at 1168/1163 cm^{-1} for PYP_H/PYP and 1169/1162 cm^{-1} for PYP_L/PYP. The 1482-cm^{-1} band for PYP in PYP_M/PYP was not observed in PYP_H/PYP and PYP_L/PYP. It would be because the intensity of this mode of PYP was similar to that of PYP_H and PYP_L and canceled the difference FTIR spectra. Unexpectedly, PYP_H/PYP and PYP_L/PYP had the ~1438-cm^{-1} mode of PYP. However, it can be explained by lower intensity of this mode in PYP_H and PYP_L than that in PYP. These findings therefore indicate that the chromophores of PYP_H and PYP_L are deprotonated.

In PYP_B/PYP, the 1168-cm^{-1} band was not observed for PYP_B, whereas the bands at 1485, 1438, and 1164 cm^{-1} were clearly observed for PYP. It was very similar to PYP_M/PYP and may at a first glance suggest that the chromophore of PYP_B is protonated. However, this is considered unlikely because (1) PYP_B had no band at 1177 cm^{-1} which demonstrates the protonation of the chromophore, (2) the absorption spectrum of PYP_B is red-shifted, and (3) the plausible proton donor, Glu46, was protonated. Therefore, it is considered that the bands were not observed because their intensities were too low. Indeed, the intensity of the bands of the cis form are sometimes weaker than those of the trans form (Figure 4).

The present experiment clearly showed that all the intermediates of PYP have chromophores in the cis configuration. The important finding is that the chromophores of PYP_H and PYP_B are in cis form like those of their thermal products (*21*−*23*, *25*). Because they are the primary intermediates of PYP, the photon absorption directly induces the isomerization of the chromophore as with retinal proteins. In the present experiment, the downshift of the 1294-cm^{-1} band was used as the indicator of the isomerization of the chromophore. However, all the difference spectra had 995-/984-cm^{-1} bands. Although these modes could not be observed in the free coumaric acid because the baseline in this region was unstable, it may indicate configuration of the chromophore.

FTIR spectroscopy provides information on the differences among the intermediates. The most clear markers to distinguish the intermediates were the modes at 1016, 995, and 967 cm^{-1} present in PYP_H/PYP. PYP_H had all three bands although that at 967 cm^{-1} was weak. PYP_L had 993- and 962-cm^{-1} bands, but PYP_B and PYP_M had only the 994-cm^{-1} band. It should be noted that these characteristic modes appearing at 1020−960 cm^{-1} were not shifted in 2,6-$^{2}H_2$-PYP, whereas they were shifted in 8-^{2}H-PYP (Figure 5). These modes thus reflected the structure of the ethylene bond region rather than the phenol part, and the structural difference between PYP_B, PYP_H, and PYP_L lies in the structure around the ethylene bond. The parallel formation of PYP_H and PYP_B is characteristic of the photocycle of PYP. Their absorption spectra were strikingly different, but the chromophores are in cis form. At 77 K, because the protein conformational change is considered to be very small, the difference between PYP_H and PYP_B is considered to originate from the chromophore, particularly in the ethylene bond region. There are three possible explanations for the difference in chromophores between PYP_H and PYP_B. First, part of the rotation is different; for example, the ester part of chromophore is flipped for formation of one intermediate and the phenol part is flipped for the other. In fact, crystallography has demonstrated that the ester part is flipped in PYP_{BL} (*23*) and the phenol part is flipped in PYP_L and PYP_M (*21*, *22*). Both parts are able to rotate in the crystal. However, this explanation is unlikely in the dry film sample because the frequency of the C═O stretching mode in PYP_H agreed with that in PYP_B. In addition, both of their absorption spectra were affected by mutation at Glu46, suggesting the presence of an interaction between the chromophore and Glu46 in PYP_H and PYP_B. Second, because there is restricted space around the chromophore, the double bond would not completely rotate in the early intermediates and the torsional angles of the ethylene bonds are different between them. Third, the direction of the rotation is different: right-hand rotation and left-hand rotation yield different photoproducts. Crystallography at liquid nitrogen temperature has not been reported, but it will be clarified by the high-resolution structural analysis.

REFERENCES

1. Meyer, T. E. (1985) *Biochim. Biophys. Acta 806*, 175−183.
2. Meyer, T. E., Fitch, J. C., Bartsch, R. G., Tollin, G., and Cusanovich, M. A. (1990) *Biochim. Biophys. Acta 1016*, 364−370.
3. Meyer, T. E., Cannac, V., Fitch, J., Bartsch, R. G., Tollin, D., Tollin, G., and Cusanovich, M. A. (1990) *Biochim. Biophys. Acta 1017*, 125−138.
4. Koh, M., Van Driessche, G., Samyn, B., Hoff, W. D., Meyer, T. E., Cusanovich, M. A., and Van Beeumen, J. J. (1996) *Biochemistry 35*, 2526−2534.
5. Kort, R., Hoff, W. D., Van West, M., Kroon, A. R., Hoffer, S. M., Vlieg, K. H., Crielaard, W., Van Beeumen, J. J., and Hellingwerf, K. J. (1996) *EMBO J. 15*, 3209−3218.
6. Kort, R., Phillips-Jones, M. K., van Aalten, D. M., Haker, A., Hoffer, S. M., Hellingwerf, K. J., and Crielaard, W. (1998) *Biochim. Biophys. Acta 1385*, 1−6.
7. Sprenger, W. W., Hoff, W. D., Armitage, J. P., and Hellingwerf, K. J. (1993) *J. Bacteriol. 175*, 3096−3104.
8. Van Beeumen, J. J., Devreese, B. V., Van Bun, S. M., Hoff, W. D., Hellingwerf, K. J., Meyer, T. E., McRee, D. E., and Cusanovich, M. A. (1993) *Protein Sci. 2*, 1114−1125.
9. Baca, M., Borgstahl, G. E. O., Boissinot, M., Burke, P. M., Williams, D. R., Slater, K. A., and Getzoff, E. D. (1994) *Biochemistry 33*, 14369−14377.

10. Hoff, W. D., Düx, P., Hård, K., Devreese, B., Nugteren-Roodzant, I. M., Crielaard, W., Boelens, R., Kaptein, R., Van Beeumen, J., and Hellingwerf, K. J. (1994) *Biochemistry 33*, 13959−13962.
11. Imamoto, Y., Ito, T., Kataoka, M., and Tokunaga, F. (1995) *FEBS Lett. 374*, 157−160.
12. Imamoto, Y., Kataoka, M., and Tokunaga, F. (1996) *Biochemistry 35*, 14047−14053.
13. Imamoto, Y., Mihara, K., Hisatomi, O., Kataoka, M., Tokunaga, F., Bojkova, N., and Yoshihara, K. (1997) *J. Biol. Chem. 272*, 12905−12908.
14. Ujj, L., Devanathan, S., Meyer, T. E., Cusanovich, M. A., Tollin, G., and Atkinson, G. H. (1998) *Biophys. J. 75*, 406−412.
15. Hoff, W. D., Van Stokkum, I. H. M., Van Ramesdonk, H. J., Van Brederode, M. E., Brouwer, A. M., Fitch, J. C., Meyer, T. E., Van Grondelle, R., and Hellingwerf, K. J. (1994) *Biophys. J. 67*, 1691−1705.
16. Meyer, T. E., Yakali, E., Cusanovich, M. A., and Tollin, G. (1987) *Biochemistry 26*, 418−423.
17. Ohishi, S., Shimizu, N., Mihara, K., Imamoto, Y., and Kataoka, M. (2001) *Biochemistry 40*, 2854−2859.
18. Imamoto, Y., Kataoka, M., Tokunaga, F., Asahi, T., and Masuhara, H. (2001) *Biochemistry 40*, 6047−6052.
19. Borgstahl, G. E. O., Williams, D. R., and Getzoff, E. D. (1995) *Biochemistry 34*, 6278−6287.
20. Düx, P., Rubinstenn, G., Vuister, G. W., Boelens, R., Mulder, F. A., Hård, K., Hoff, W. D., Kroon, A. R., Crielaard, W., Hellingwerf, K. J., and Kaptein, R. (1998) *Biochemistry 37*, 12689−12699.
21. Genick, U. K., Borgstahl, G. E., Ng, K., Ren, Z., Pradervand, C., Burke, P. M., Srajer, V., Teng, T. Y., Schildkamp, W., McRee, D. E., Moffat, K., and Getzoff, E. D. (1997) *Science 275*, 1471−1475.
22. Perman, B., Šrajer, V., Ren, Z., Teng, T., Pradervand, C., Ursby, T., Bourgeois, D., Schotte, F., Wulff, M., Kort, R., Hellingwerf, K., and Moffat, K. (1998) *Science 279*, 1946−1950.
23. Genick, U. K., Soltis, S. M., Kuhn, P., Canestrelli, I. L., and Getzoff, E. D. (1998) *Nature 392*, 206−209.
24. Rubinstenn, G., Vuister, G. W., Mulder, F. A., Düx, P. E., Boelens, R., Hellingwerf, K. J., and Kaptein, R. (1998) *Nat. Struct. Biol. 5*, 568−570.
25. Kort, R., Vonk, H., Xu, X., Hoff, W. D., Crielaard, W., and Hellingwerf, K. J. (1996) *FEBS Lett. 382*, 73−78.
26. Brudler, R., Rammelsberg, R., Woo, T. T., Getzoff, E. D., and Gerwert, K. (2001) *Nat. Struct. Biol. 8*, 265−270.
27. Xie, A., Kelemen, L., Hendriks, J., White, B. J., Hellingwerf, K. J., and Hoff, W. D. (2001) *Biochemistry 40*, 1510−1517.
28. Braiman, M. S., Mogi, T., Marti, T., Stern, L. J., Khorana, H. G., and Rothschild, K. J. (1988) *Biochemistry 27*, 8516−8520.
29. Maeda, A. (1995) *Isr. J. Chem. 35*, 387−400.
30. Hoff, W. D., Xie, A., Van Stokkum, I. H., Tang, X. J., Gural, J., Kroon, A. R., and Hellingwerf, K. J. (1999) *Biochemistry 38*, 1009−1017.
31. Xie, A., Hoff., W. D., Kroon, A. R., and Hellingwerf, K. J. (1996) *Biochemistry 35*, 14671−14678.
32. Kandori, H., Iwata, T., Hendriks, J., Maeda, A., and Hellingwerf, K. J. (2000) *Biochemistry 39*, 7902−7909.
33. Mihara, K., Hisatomi, O., Imamoto, Y., Kataoka, M., and Tokunaga, F. (1997) *J. Biochem. (Tokyo) 121*, 876−880.
34. Meyer, T. E., Tollin, G., Hazzard, J. H., and Cusanovich, M. A. (1989) *Biophys. J. 56*, 559−564.
35. Genick, U. K., Devanathan, S., Meyer, T. E., Canestrelli, I. L., Williams, E., Cusanovich, M. A., Tollin, G., and Getzoff, E. D. (1997) *Biochemistry 36*, 8−14.
36. Imamoto, Y., Koshimizu, H., Mihara, K., Hisatomi, O., Mizukami, T., Tsujimoto, K., Kataoka, M., and Tokunaga, F. (2001) *Biochemistry 40*, 4679−4685.
37. Kim, M., Mathies, R. A., Hoff, W. D., and Hellingwerf, K. J. (1995) *Biochemistry 34*, 12669−12672.

BI010021L